



Crosslinked amino starch prepared via a dry process and its decoloration performance of Congo Red

Lei Guo*, Kaijin Jin, Yuanchao Cao, Guiying Li, Junshen Liu

School of Chemistry and Materials Science, Ludong University, Yantai 264025, China, Tel. +86-535-6672176; Fax: +86-535-6696162; emails: unikguo@gmail.com (L. Guo), 1047678508@qq.com (K. Jin), 1076197425@qq.com (Y. Cao), 26362442@qq.com (G. Li), xincaihuanbao@qq.com (J. Liu)

Received 30 October 2018; Accepted 8 March 2019

ABSTRACT

Three types of crosslinked amino starch (CAS) were prepared via a dry process by using monomethylamine, dimethylamine and trimethylamine as materials, respectively. The effect of material ratio on the nitrogen content of CAS was investigated. CASs were characterized by scanning electron microscopy and Fourier-transform infrared spectroscopy. The decoloration performance of Congo Red in the aqueous solution by CASs was also studied. With the aim to understand the adsorption mechanism and evaluate the maximum adsorption capacity, the adsorption equilibrium data were analyzed by Langmuir, Freundlich and Sips models. The isotherm data fits the Sips model better than the others. The maximum adsorption capacities of crosslinked monomethylamine starch, crosslinked dimethylamine starch and crosslinked trimethylamine starch are 363.09, 243.62 and 358.46 mg/g, respectively.

Keywords: Crosslinked amino starch; Dry process; Decoloration; Congo red; Isotherm

1. Introduction

Synthetic dyes, as common industrial raw materials, have been widely used in different industries such as textiles, paper, plastics and leather. It is estimated that 10%–15% of the total dye produced is discharged into the environment in effluent [1]. Most of the dyes contain aromatic rings in their structures, which make them non-biodegradable, carcinogenic and mutagenic for aquatic systems and human health [2]. Therefore, removing them from the aquatic ecosystems is essential. A variety of physical and chemical methods are applied to dye treatment, such as flocculation [3], adsorption [4], photodegradation [5], electrochemical oxidation [6] and biodegradation [7]. Adsorption has been considered as the attractive technology, due to its simple operation, without secondary pollution, low cost and high removal efficiency [8].

As an abundant, inexpensive, environmental friendly and biodegradable material, starch is suitable to prepare adsorbents [9,10]. Recently, starch-based materials are widely studied to adsorb synthetic dyes from aqueous solution [11]. Delval et al. [12] prepared amino starches using epichlorohydrin and NH_4OH as crosslinking agents and used them to adsorb various dyes from aqueous solutions. The results showed that amino starch exhibited interesting sorption properties and that the sorption mechanism was correlated to the structure of the polymer. Gomes et al. [13] prepared starch/cellulose nanowhiskers hydrogel composite and used them as robust and efficient methylene blue adsorbent. He et al. [14] prepared chitosan/oxidized starch/silica hybrid membrane by using oxidized starch and 3-aminopropyltriethoxysilane as crosslinking agents and studied its adsorption properties for two direct dyes (Blue 71 and Red 31). In the development of adsorbents, high

* Corresponding author.

adsorption efficiency as well as a green and simple process are the most two important aspects.

In this work, three kinds of crosslinked amino starch (CAS) were prepared via a dry process by using monomethylamine (MMA), dimethylamine (DMA) and trimethylamine (TMA) as materials, respectively. Effect of the materials ratio on the nitrogen content of CAS was studied. In the preparation of starch derivatives, dry process is known as green and simple process due to high degree of substitution, high reaction efficiency, pollution-free, without gelatinization inhibitors, etc. [15]. Because of the cationic character of CAS, CAS may show good adsorption performance to some anionic dyes by electrostatic interaction. Congo red (CR) is a benzidine-based anionic bisazo dye, which is acknowledged to metabolize to benzidine [16]. Then CR, as a model dye, was used to evaluate the adsorption performance of CAS to anionic dyes. With the aim to understand the adsorption mechanism and evaluate the maximum adsorption capacity, the isotherms models were used to analyze the adsorption equilibrium data.

2. Materials and methods

2.1. Materials

Corn starch (Food grade), purchased from Zhucheng Xingmao Corn Developing Co., Ltd. (Weifang, China), was dried at 105°C before it was used. The CR and sodium hydroxide were analytical grade and provided by Sinopharm Reagent chemicals Co., Ltd. (Shanghai, China). The monomethylamine, dimethylamine and trimethylamine were all analytical grade and obtained from Tianjin Fuchen Chemical Reagents Factory (Tianjin, China). Epichlorohydrin (ECH, Analytical grade) was obtained from Tianjin Bodi Chemical Co., Ltd. (Tianjin, China). All other commercial chemicals were analytical grade and used without further purification. The water used in all the experiments was doubly distilled.

2.2. Synthesis of CAS

CAS was prepared in two steps via a dry process. Corn starch was activated with NaOH, and then CAS was prepared by reacting active starch with ECH and amine. A typical crosslinking reaction was carried out as follows: Corn starch (16.2 g, dried) was mixed with NaOH (4 g, 50% W/W) to give a homogeneous paste via a high-speed mixer (Philips HR2874, China). The mixture was heated at 45°C for 2 h in an oven. After cooling to room temperature, the activated starch was mixed with ECH and MMA to give a homogeneous paste via a high-speed mixer (Philips HR2874, China). The mole ratio of starch, ECH and MMA were 0.1:0.015:0.01, 0.1:0.03:0.02 and 0.1:0.075:0.05, as shown in Table 1. Then the mixture was heated in an oven at 50°C for 5 h. Finally, the products were washed with distilled water for three times and then dried at 50°C for 12 h. The samples are named as crosslinked monomethylamine starch (CMS).

Crosslinked dimethylamine starch (CDS) and cross-linked trimethylamine starch (CTS) were prepared under the same conditions by using DMA and TMA instead of MMA, respectively.

Table 1
Effect of molar ratio of raw materials on the nitrogen content of products

	The material mole ratio	Nitrogen content (mmol/g)
	$n_{\text{starch}}:n_{\text{ECH}}:n_{\text{MMA}}$	
CMS1	0.1:0.015:0.01	0.24
CMS2	0.1:0.03:0.02	0.33
CMS3	0.1:0.075:0.05	0.68
	$n_{\text{starch}}:n_{\text{ECH}}:n_{\text{DMA}}$	
CDS1	0.1:0.015:0.01	0.17
CDS2	0.1:0.03:0.02	0.26
CDS3	0.1:0.075:0.05	0.59
	$n_{\text{starch}}:n_{\text{ECH}}:n_{\text{TMA}}$	
CTS1	0.1:0.015:0.01	0.13
CTS2	0.1:0.03:0.02	0.21
CTS3	0.1:0.075:0.05	0.44

2.3. Characterization of samples

Nitrogen contents of samples were measured by the Kjeldahl method (ISO 3188: 1978). The surface morphology of raw starch (RS), CMS, CDS and CTS were characterized by a scanning electron microscopy (JSM-5610LV, Jeol, Japan). The information of Fourier Transform Infrared (FTIR) was obtained on FTIR spectrometer (MAGNA550, Nicolet, America) with samples in KBr pellets and wavenumber over the range of 400–4,000 cm^{-1} at 25°C.

2.4. Batch adsorption experiments of CR

Batch methods were adopted in the adsorption experiments. A series of CR solution with the concentration from 0 to 3,000 mg/L. The initial pH of CR solution was adjusted to 6.0 by adding either 0.1 M HCl solution or 0.1 M NaOH solution. 50 mg of CAS was added to 50 mL of CR aqueous solution in a 100 mL glass-stoppered Erlenmeyer flask. The suspension was stirred at a uniform speed of 120 rpm on a water bath oscillator (SHA-C, China) at room temperature. After the equilibrium was reached (about 180 min), the suspension was filtered through a 0.2 μm nylon membrane by using a syringe filter, and the concentration of CR in the aqueous phase was determined by using a Shimadzu UV-VIS spectrophotometer (UV-2550, Japan) at the maximum wavelength of 500 nm. Repeated three times in each cases. The adsorption capacity was calculated according to Eq. (1):

$$Q = \frac{(C_i - C_f)V}{m} \quad (1)$$

where Q is the adsorption capacity of CR (mg/g), C_i and C_f (mg/L) are the initial and final concentrations of the CR in the adsorption solution, respectively. V (mL) is the volume of the adsorption solution and m (mg) is the mass of the adsorbent.

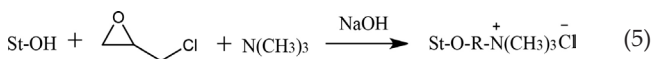
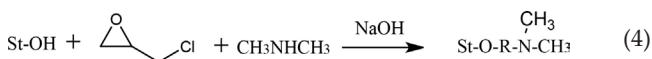
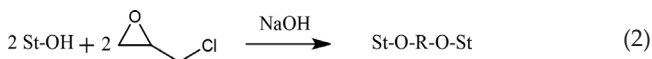
3. Results and discussion

3.1 Preparation of CAS and their characterization

3.1.1 Preparation of CAS

The preparation of CAS was carried out as a baking process. The effect of molar ratio of materials on the nitrogen content of CAS is presented in Table 1. Generally, the nitrogen content gradually increases with increasing amount of ECH and amine. This can be explained by a more intensive crosslinking reaction. The comparison among CMS, CDS and CTS turns out that they show different reaction trends. At the same molar ratio of materials, the nitrogen content of CMS, CDS and CTS were reduced in turn. The reason may be the steric hindrance of amine.

ECH is the most common crosslinker in the preparation of crosslinked starch [17]. Excess ECH, about 1.5 times the amount of amine, was used in the present study to improve the mechanical stability of CAS. Simkovic et al. prepared crosslinked starch in one step via the crosslinking of starch with ECH and NH_4OH [18]. As described by Simkovic, a poly(hydroxypropylamine)-based material could be produced by reacting only ECH with NH_4OH in a basic media [18]. According to Simkovic's opinions, a possible reaction mechanism of starch, ECH and amine is shown in Fig. 1. The main reaction of starch, ECH and MMA is Eq. (3). The main reaction of starch, ECH and DMA is Eqs. (2) and (4). The main reaction of starch, ECH and TMA is Eqs. (2) and (5).



3.1.2. FTIR spectra analysis

The FTIR spectra of CTS, CDS, CMS and RS are shown in Fig. 2. The broad absorption peaks around 3400 cm^{-1} are indicative of the existence of bonded hydroxyl groups. The peaks of modified starch are broadened because of the hydroxyl groups that are reacted. Bands at 2920 cm^{-1} attribute to the C-H stretching vibration. The characteristic ring vibrations and the especially anomeric C-H deformations are still present in the polymers in the $900\text{--}550 \text{ cm}^{-1}$ region [19]. In the IR spectra of CAS, the band at $2,854 \text{ cm}^{-1}$ appears corresponding to C-H (in CH_2N group) vibrations, which indicates amine is introduced in CAS.



Fig. 1. A possible reaction mechanism of starch, ECH and amine.

3.1.3 SEM analysis

The scanning electron micrographs of RS, CMS, CDS and CTS are shown in Fig. 3. As can be seen, the RS granules are almost spherically shaped, with a smooth surface. The size of the granules is about $10 \mu\text{m}$. After reacting with ECH and amine, the surface of the CAS particles are rough and have multiple collapses, leading to an increase in its specific surface area. Solid-phase reactions usually occur on the surface of the starch granules, often accompanied by the deformation of the granules. Crosslinked starch phosphate carbamates using a dry process shows the similar morphology with CAS [20].

Compared CDS and CTS with CMS, the surface morphology is different. The surface of the CMS particles was rougher and the holes were smaller. The changes in morphology may be due to the difference of crosslinking mechanism. The crosslinking of CMS is mainly Eq. (3). The crosslinking of CDS and CTS are mainly Eq. (2). A more intensive crosslinking reaction leads to rougher surface and smaller holes on the CMS granules.

3.2. Adsorption performance of CR on CAS

As a model dye, CR was used to evaluate the adsorption performance of CAS to anionic dyes. Nine CAS samples, as shown in Table 1, were used to adsorb CR via batch methods at room temperature. Effect of the equilibrium concentration on the adsorption capacities of CR on CAS is shown in Fig. 4 as dots.

All of the samples depict the similar phenomenon: the adsorption capacity increases rapidly with the increase of CR concentration, then the adsorption capacity increases slightly until the equilibrium is reached. The content of nitrogen has a significant effect on the adsorption capacity. Fig. 4(a) shows that the maximum adsorption capacity of CMS1 from the experiments is 145.59 mg/g at the equilibrium concentration of $2,854.41 \text{ mg/L}$. The equilibrium concentration at the saturated adsorption does not change much for the adsorption of CR on CMS2, but the adsorption capacity increases to 194.6 mg/g . With the increase of nitrogen content,

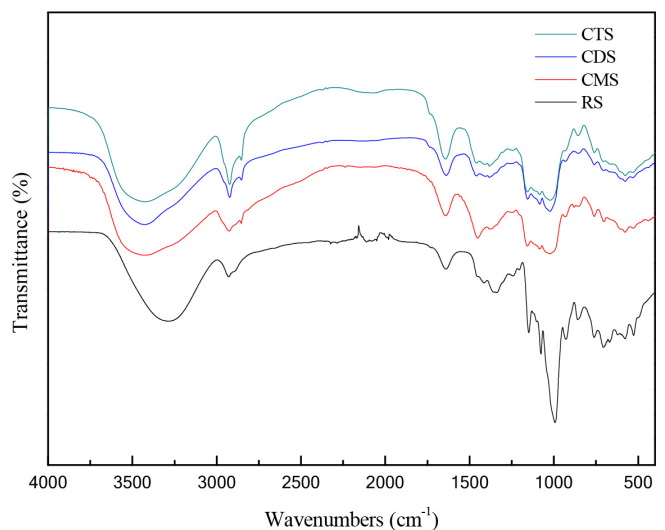


Fig. 2. FTIR spectra of CTS, CDS, CMS and RS.

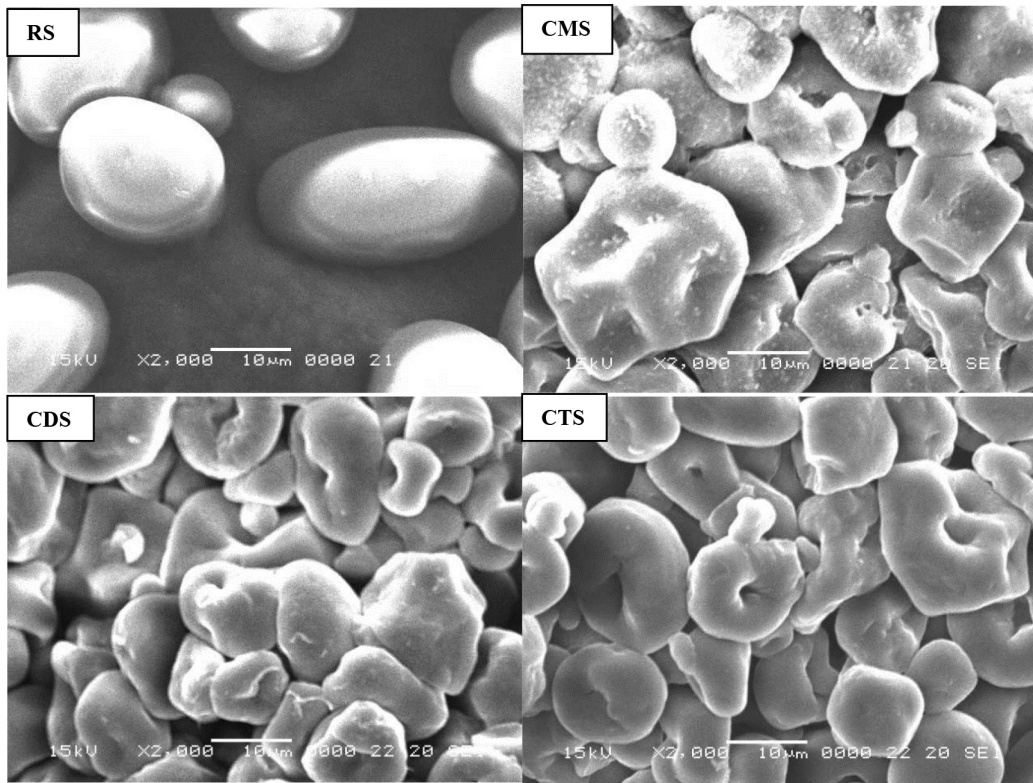


Fig. 3. The SEM images of RS, CMS, CDS and CTS.

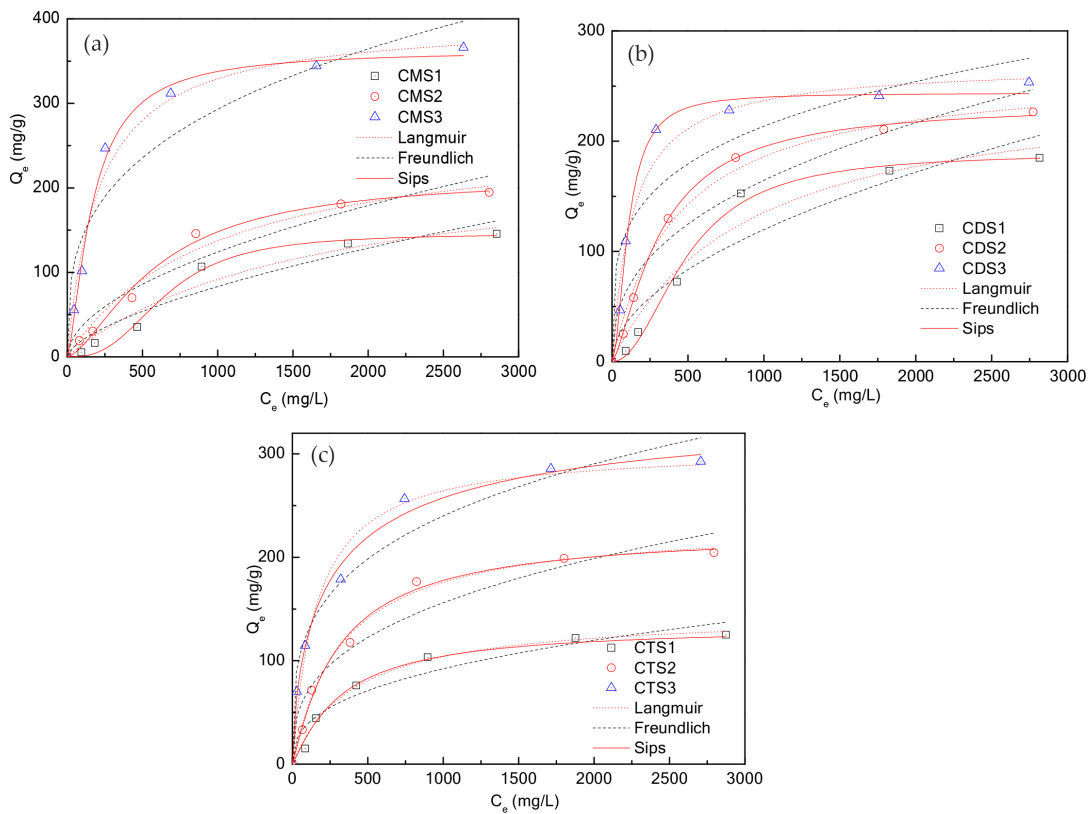


Fig. 4. Effect of the equilibrium concentration on the adsorption capacities of CR on CMS (a), CDS (b) and CTS (c) and adsorption equilibrium isotherms.

the maximum adsorption capacity increases dramatically. The equilibrium adsorption capacity rises to 366.17 mg/g at the equilibrium concentration of 2,633.83 mg/L for the adsorption of CR on CMS3. The similar trend is also found in Fig. 4(b) (for the adsorption of CR on CDS) and Fig. 4(c) (for the adsorption of CR on CTS). The maximum adsorption capacity of CR on CDS and CTS from the experiments are 253.44 and 292.64 mg/g, respectively. The increase in nitrogen content indicates an increase in the content of amino groups in CAS, providing more active sites for the adsorption of CR. On comparing the adsorption capacities of CMS, CDS and CTS, CMS3 shows the highest adsorption capacity because of its highest nitrogen content. Though the nitrogen content of CTS3 is lower than the CMS3 and CDS3, CTS3 shows the second highest adsorption capacity. This is owing to the cationic nature of CTS3, as shown in Fig. 1. CTS3 shows excellent adsorption performance to CR by electrostatic interaction due to its relatively strong cationic character.

Isotherm modeling is an indispensable tool to understand the adsorption mechanism and evaluate the maximum

adsorption capacity. Langmuir [21], Freundlich [22] and Sips [23] isotherms were widely used to examine the importance of different factors on dyes adsorption by a given adsorbent, and then the three isotherms have been used to describe the experimental data for the equilibrium adsorption of CR on CAS.

The equations of Langmuir, Freundlich and Sips isotherms are summarized in Table 2. In the three equations, C_e and Q_e are equilibrium CR concentration (mg/L) and equilibrium adsorption capacity (mg/g), respectively; Q_m is the constant representing maximum adsorption capacity (mg/g). The parametric values of the respective isotherms have been obtained by using non-linear regression analyses and are given in Table 3. The maximum adsorption capacity from the experiments (Q_{m-exp}) is also shown in Table 3. The plots in Figs. 4(a)–(c) are the isotherms for the adsorption of CR on CMS, CDS and CTS, respectively.

Comparing the correlation coefficients (R^2), Sips isotherm ($R^2 > 0.99$) is the best-fit isotherm among the three isotherm models for all the nine samples. Sips isotherm is the combination of both Langmuir and Freundlich isotherms. At low adsorbate concentrations, it reduces to a Freundlich isotherm, while at high adsorbate concentrations it shows the characteristic of the Langmuir isotherm with a saturated adsorption capacity. The maximum adsorption capacities of CMS3, CDS3 and CTS3 from Sips isotherm fitting are 363.09, 243.62 and 358.46 mg/g, respectively. For the results presented in Table 3, the Sips isotherm provided accurate fit to the experimental data. The Sips model exponent s indicates surface heterogeneity and for a highly heterogeneous system, the deviation of s value from unity will be higher. The s values of CMS and CDS show higher deviation from unity than CTS, which indicates that the CMS and CDS surfaces are more heterogeneous than CTS in nature. The surface heterogeneity of CMS and CDS may be attributed to the crosslinking reactions, as shown in Fig. 1. The adsorption of CR on other amino biomaterials such as cross-linked chitosan [24] and gemini surfactant modified chitosan hydrogel beads [25] were also observed to obey Sips equation well.

Table 2
The summary of adsorption isotherms

Isotherm	Equation	Parameters
Langmuir	$Q_e = \frac{Q_m K_L C_e}{1 + K_L C_e}$	K_L : the Langmuir equilibrium constant related to adsorption affinity, L/mg
Freundlich	$Q_e = K_F C_e^{1/n}$	K_F : the Freundlich constant related to the adsorption capacity, (mg/g)(L/mg) ^{1/n} ; n , the Freundlich constant related to adsorption intensity
Sips	$Q_e = \frac{Q_m (K_S C_e)^{1/s}}{1 + (K_S C_e)^{1/s}}$	K_S : the Sips equilibrium constant related to adsorption affinity, L/mg; s : the heterogeneity factor

Table 3
Adsorption isotherm model constants and correlation coefficients for the adsorption of CR on CAS

Parameters	CMS1	CMS2	CMS3	CDS1	CDS2	CDS3	CTS1	CTS2	CTS3
Langmuir									
Q_m (mg/g)	239.48	273.35	398.73	256.08	266.45	269.42	146.40	233.71	306.47
K_L (10 ⁻³ L/mg)	0.62	1.01	4.73	1.12	2.31	7.28	2.46	3.04	6.28
R^2	0.9618	0.9832	0.9869	0.9678	0.9921	0.9747	0.9914	0.9939	0.9853
Freundlich									
K_F ((mg/g)(L/mg) ^{1/n})	1.08	3.21	33.38	3.28	10.49	37.64	6.87	13.94	35.98
n	1.59	1.89	3.18	1.92	2.51	3.98	2.66	2.86	3.64
R^2	0.928	0.9487	0.916	0.9149	0.9364	0.885	0.9406	0.9479	0.9701
Sips									
Q_m (mg/g)	145.82	214.2	363.09	189.32	233.71	243.62	133.78	226.42	358.46
K_S (10 ⁻³ L/mg)	1.53	1.69	5.97	2.04	3.15	9.41	3.07	3.29	3.89
s	0.36	0.65	0.69	0.48	0.71	0.54	0.80	0.92	1.45
R^2	0.9922	0.9962	0.9952	0.9938	0.9993	0.9958	0.9945	0.9944	0.9937
Q_{m-exp} (mg/g)	145.59	194.6	366.17	184.8	226.52	253.44	125.07	204.46	292.64

Table 4
Comparative assessment of CAS as an adsorbent of CR with already reported materials

Adsorbents	Isotherm	Q_m (mg/g)
Cetyltrimethyl ammonium bromide modified hectorite [26]	Langmuir	182
Octadecylamine modified hectorite [26]	Langmuir	197
MnFe ₂ O ₄ /PW [27]	Langmuir	86.96
Cationic modified orange peel powder [28]	Langmuir	163
ZnO-modified SiO ₂ nanospheres [29]	Langmuir	90.1
MgO-graphene oxide composites [30]	Langmuir	237.0
MgO microspheres [30]	Langmuir	227.7
Chitosan hydrobeads [31]	Langmuir	93.40
Apricot stone activated carbon [32]	Temkin	32.85
Fe ₃ O ₄ /Bi ₂ S ₃ microspheres [33]	Langmuir	90.58
Polypyrrole–polyaniline nanofibres [34]	Langmuir	270.27
N,N-dimethyl dehydroabietylamine oxide [35]	Langmuir	69.94
Crosslinked cellulose dialdehyde [36]	Langmuir	34.7
NiAl layered double hydroxides [37]	Langmuir	120.5
Diammonium tartrate modified chitosan [24]	Sips	1,597
Urea diammonium tartrate modified chitosan [24]	Sips	1,447
Chitosan beads [25]	Sips	1,260
Gemini surfactant modified chitosan hydrogel [25]	Sips	2,192
CMS3	Sips	363.09

3.3. Comparative assessment of CAS as an adsorbent of CR

The performance of CAS has been compared with the related adsorbents which are reported previously which is represented in Table 4. The maximum adsorption capacity is from the Langmuir, Sips or Temkin isotherm fitting. Comparison of CMS3 with different adsorbents shows that CMS3 has a higher adsorption capacity than other adsorbents except for modified chitosan materials.

4. Conclusion

Three types of CAS were successfully prepared via a dry process by using MMA, DMA and TMA as materials. The results of FTIR spectra and SEM indicate the crosslinking reaction mechanism. The nitrogen content gradually increases with increasing amount of ECH and amine due to a more intensive crosslinking reaction. At the same molar ratio of materials, the nitrogen content of CMS, CDS and CTS were reduced in turn because of the steric hindrance of amine. CAS has good decoloration performance of CR. The decoloration performance is highly affected by the nitrogen content and type of CAS. Results show that the higher the nitrogen content of CAS, the greater the adsorption capacity. The equilibrium data were analyzed by Langmuir, Freundlich and Sips isotherm. The equilibrium data fit Sips isotherm better than the others and the maximum adsorption capacity of CMS, CDS and CTS is 363.09, 243.62 and 358.46 mg/g, respectively. CAS has a promising future for the CR removal from the effluent.

Acknowledgements

These authors acknowledged the National Natural Science Foundation of China (21206066), National Key

Technology R&D Program (2015BAB02B03) and the Natural Science Foundation of Shandong Province (ZR2018PB013).

References

- [1] K.H. Gonawala, M.J. Mehta, Removal of color from different dye wastewater by using ferric oxide as an adsorbent, *Int. J. Eng. Res. Appl.*, 4 (2014) 102–109.
- [2] H. Hou, R. Zhou, P. Wu, L. Wu, Removal of congo red dye from aqueous solution with hydroxyapatite/chitosan composite, *Chem. Eng. J.*, 211 (2012) 336–342.
- [3] V. Golob, A. Vinder, M. Simonič, Efficiency of the coagulation/flocculation method for the treatment of dyebath effluents, *Dyes Pigments*, 67 (2005) 93–97.
- [4] V. Gupta, A. Mittal, L. Krishnan, J. Mittal, Adsorption treatment and recovery of the hazardous dye, brilliant blue FCF, over bottom ash and de-oiled soya, *J. Colloid Interface Sci.*, 293 (2006) 16–26.
- [5] V.K. Gupta, R. Jain, A. Nayak, S. Agarwal, M. Shrivastava, Removal of the hazardous dye—tartrazine by photodegradation on titanium dioxide surface, *Mat. Sci. Eng. C*, 31 (2011) 1062–1067.
- [6] N. Mohan, N. Balasubramanian, C.A. Basha, Electrochemical oxidation of textile wastewater and its reuse, *J. Hazard. Mater.*, 147 (2007) 644–651.
- [7] E. Franciscon, A. Zille, F. Dias Guimaro, C. Ragagnin de Menezes, L.R. Durrant, A. Cavaco-Paulo, Biodegradation of textile azo dyes by a facultative *Staphylococcus arlettae* strain VN-11 using a sequential microaerophilic/aerobic process, *Int. Biodeter. Biodegr.*, 63 (2009) 280–288.
- [8] M.T. Yagub, T.K. Sen, S. Afroze, H.M. Ang, Dye and its removal from aqueous solution by adsorption: a review, *Adv. Colloid Interface Sci.*, 209 (2014) 172–184.
- [9] L. Guo, Y. Cao, G. Li, J. Liu, L. Han, H. Zhang, Preparation of starch sulfate resin and its adsorption performance for malachite green, *Desalin. Wat. Treat.*, 97 (2017) 321–328.
- [10] L. Guo, C. Sun, G. Li, C. Liu, C. Ji, Thermodynamics and kinetics of Zn(II) adsorption on crosslinked starch phosphates, *J. Hazard. Mater.*, 161 (2009) 510–515.
- [11] F. Renault, N. Morin-Crini, F. Gimbert, P.M. Badot, G. Crini, Cationized starch-based material as a new ion-exchanger

- adsorbent for the removal of CI acid blue 25 from aqueous solutions, *Bioresour. Technol.*, 99 (2008) 7573–7586.
- [12] F. Delval, G. Crini, S. Bertini, C. Filiatre, G. Torri, Preparation, characterization and sorption properties of crosslinked starch-based exchangers, *Carbohydr. Polym.*, 60 (2005) 67–75.
- [13] R.F. Gomes, A.C.N. de Azevedo, A.G.B. Pereira, E.C. Muniz, A.R. Fajardo, F.H.A. Rodrigues, Fast dye removal from water by starch-based nanocomposites, *J. Colloid Interface Sci.*, 454 (2015) 200–209.
- [14] X. He, M. Du, H. Li, T. Zhou, Removal of direct dyes from aqueous solution by oxidized starch cross-linked chitosan/silica hybrid membrane, *Int. J. Biol. Macromol.*, 82 (2016) 174–181.
- [15] M. Zhang, B.Z. Ju, S.F. Zhang, W. Ma, J.Z. Yang, Synthesis of cationic hydrolyzed starch with high DS by dry process and use in salt-free dyeing, *Carbohydr. Polym.*, 69 (2007) 123–129.
- [16] K. Hunger, P. Mischke, W. Rieper, R. Raue, K. Kunde, A. Engel, *Azo Dyes*, Ullmann's Encyclopedia of Industrial Chemistry, Wiley-VCH Verlag, GmbH & Co. KGaA, 2000.
- [17] L. Kuniak, R. Marchessault, Study of the crosslinking reaction between epichlorohydrin and starch, *Starch*, 24 (1972) 110–116.
- [18] I. Šimković, J.A. Laszlo, A.R. Thompson, Preparation of a weakly basic ion exchanger by crosslinking starch with epichlorohydrin in the presence of NH_4OH , *Carbohydr. Polym.*, 30 (1996) 25–30.
- [19] F. Delval, G. Crini, N. Morin, J. Vebrel, S. Bertini, G. Torri, The sorption of several types of dye on crosslinked polysaccharides derivatives, *Dyes Pigments*, 53 (2002) 79–92.
- [20] L. Guo, S.F. Zhang, B.Z. Ju, J.Z. Yang, Study on adsorption of Cu(II) by water-insoluble starch phosphate carbamate, *Carbohydr. Polym.*, 63 (2006) 487–492.
- [21] I. Langmuir, The constitution and fundamental properties of solids and liquids. Part I. solids, *J. Am. Chem. Soc.*, 38 (1916) 2221–2295.
- [22] H. Freundlich, Over the adsorption in solution, *J. Phys. Chem.*, 57 (1906) 385–470.
- [23] R. Sips, On the structure of a catalyst surface, *J. Chem. Phys.*, 16 (1948) 490–495.
- [24] A. Zahir, Z. Aslam, M.S. Kamal, W. Ahmad, A. Abbas, R.A. Shawabkeh, Development of novel cross-linked chitosan for the removal of anionic congo red dye, *J. Mol. Liq.*, 244 (2017) 211–218.
- [25] C. Lin, S. Li, M. Chen, R. Jiang, Removal of congo red dye by gemini surfactant $\text{C}_{12}\text{-4-C}_{12}\text{-2Br}$ -modified chitosan hydrogel beads, *J. Dispersion. Sci. Technol.*, 38 (2017) 46–57.
- [26] C. Xia, Y. Jing, Y. Jia, D. Yue, J. Ma, X. Yin, Adsorption properties of congo red from aqueous solution on modified hectorite: kinetic and thermodynamic studies, *Desalination*, 265 (2011) 81–87.
- [27] G.A. Saygılı, Synthesis, characterization and adsorption properties of a novel biomagnetic composite for the removal of congo red from aqueous medium, *J. Mol. Liq.*, 211 (2015) 515–526.
- [28] V.S. Munagapati, D.S. Kim, Adsorption of anionic azo dye congo red from aqueous solution by cationic modified orange peel powder, *J. Mol. Liq.*, 220 (2016) 540–548.
- [29] J. Zhang, X. Yan, M. Hu, X. Hu, M. Zhou, Adsorption of congo red from aqueous solution using ZnO-modified SiO_2 nanospheres with rough surfaces, *J. Mol. Liq.*, 249 (2018) 772–778.
- [30] J. Xu, D. Xu, B. Zhu, B. Cheng, C. Jiang, Adsorptive removal of an anionic dye congo red by flower-like hierarchical magnesium oxide (MgO)-graphene oxide composite microspheres, *Appl. Surf. Sci.*, 435 (2018) 1136–1142.
- [31] S. Chatterjee, S. Chatterjee, B.P. Chatterjee, A.K. Guha, Adsorptive removal of congo red, a carcinogenic textile dye by chitosan hydrobeads: Binding mechanism, equilibrium and kinetics, *Colloid. Surf. A.*, 299 (2007) 146–152.
- [32] M. Abbas, M. Trari, Kinetic, equilibrium and thermodynamic study on the removal of congo red from aqueous solutions by adsorption onto apricot stone, *Process Saf. Environ. Prot.*, 98 (2015) 424–436.
- [33] H. Zhu, R. Jiang, J. Li, Y. Fu, S. Jiang, J. Yao, Magnetically recyclable $\text{Fe}_3\text{O}_4/\text{Bi}_2\text{S}_3$ microspheres for effective removal of congo red dye by simultaneous adsorption and photocatalytic regeneration, *Sep. Purif. Technol.*, 179 (2017) 184–193.
- [34] M. Bhaumik, R. McCrindle, A. Maity, Efficient removal of congo red from aqueous solutions by adsorption onto interconnected polypyrrole–polyaniline nanofibres, *Chem. Eng. J.*, 228 (2013) 506–515.
- [35] S. Liu, Y. Ding, P. Li, K. Diao, X. Tan, F. Lei, Y. Zhan, Q. Li, B. Huang, Z. Huang, Adsorption of the anionic dye congo red from aqueous solution onto natural zeolites modified with N,N-dimethyl dehydroabietylamine oxide, *Chem. Eng. J.*, 248 (2014) 135–144.
- [36] S. Kumari, D. Mankotia, G.S. Chauhan, Crosslinked cellulose dialdehyde for congo red removal from its aqueous solutions, *J. Environ. Chem. Eng.*, 4 (2016) 1126–1136.
- [37] D. Bharali, R.C. Deka, Adsorptive removal of congo red from aqueous solution by sonochemically synthesized NiAl layered double hydroxide, *J. Environ. Chem. Eng.*, 5 (2017) 2056–2067.